Passive Elimination of Polarization Sensitivity of Fiber-Optic Microwave Modulators

R. D. Esman, *Member, IEEE,* and M. J. Marrone

Abstract—**The polarization sensitivity of a bidirectional fiber-optic modulator is passively eliminated by incorporating the modulator in an orthoconjugate loop mirror or in an in-line fiber loop. We describe and analyze these fiber loop configurations which allow remote interrogation of polarization-sensitive devices with either one or two conventional singlemode fibers. For bulk single-drive modulators, the polarization sensitivity is reduced to ±0.15 dB out to 2 GHz. By utilizing a balanced, dual-drive feed to a bidirectional traveling-wave modulator, residual polarization sensitivity of ±2 dB is demonstrated for ultrawideband operation to 25 GHz and ±0.3 dB for narrowbands.**

I. Introduction

MANY TYPES of modulators in fiber-optic systems exhibit a strong dependence of the modulation on the input state of polarization (SOP). The consequences are changes in responsivity and leads to distortion and polarization fading of the sensed signal [1]. The schemes which have been devised to overcome the effects of polarization changes include active input polarization control [2]–[5], source polarization scrambling [6]–[9], depolarized sources [10], [11], and use of polarization maintaining fiber (PMF). Recently, we reported a passive scheme to address low-frequency modulators over conventional fiber links [12]. The configuration, termed an orthoconjugating loop mirror (OCLM), uses a polarization beam splitter (PBS) with the fibers from the output ports connected in a loop that contains a 90° Faraday rotator. Here we present the Jones Matrix analysis and expand the technique to include ultrawideband dual-feed traveling-wave devices.

II. OCLM and SPL

The operation of the OCLM [Fig. 1(a)] is described as follows. A linear SOP enters PBS1 and is transmitted via a conventional singlemode fiber (SMF) to PBS2. The evolution of the SOP along the SMF results in an arbitrary and time varying SOP at the input (port 1) to PBS2. The PBS2 separates the input SOP into p and s components which are directed to ports 2 and 3, respectively. The output ports of PBS2 are coupled to PMF's joined to form a loop in which the birefringence axes of the two fibers are aligned. Each of the circulating components reenters PBS2 with a SOP that exits the 4th port. However, by inserting a 90° Faraday rotator (FR) within the loop, the counterpropagating beams within the FR reenter the loop fibers on the opposite birefringence axis. Now each circulating component exits PBS2 at the original input port 1. Furthermore, analysis of this configuration shows that the return SOP is orthogonal to the input SOP. In this respect the OCLM is equivalent to a 45° FR and mirror [13]. Because of the reciprocal birefringence property of fibers [14], the SOP reentering PBS1 at port 3 is orthogonal to the SOP which exited this port and consequently the light is diverted to port 2. For proper operation, the system round-trip delays must be less than the characteristic times (~100 μs) associated with variations (typically acoustic effects) in the fiber birefringence; hence, one-way fiber lengths are limited to about 10 km.

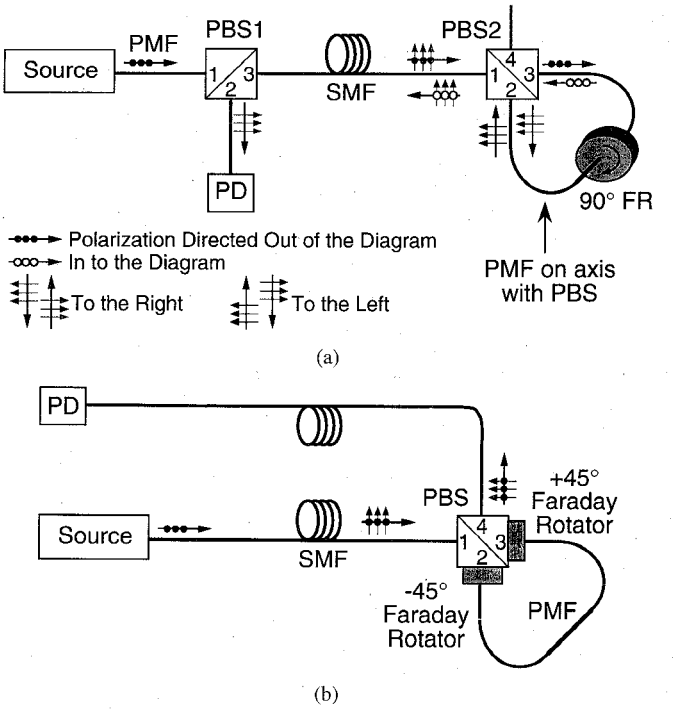

Fig. 1. Configurations to eliminate polarization sensitivity of a transducer using a single input-output fiber (a) and two separate input and output singlemode fiber (b). (a) Orthoconjugate loop mirror; loop SOP's shown for linear input SOP 45° from "Out" & 45° from "Left" of the diagram. (b) Single polarization loop; loop PMF oriented 45° off PBS axis; SOP (not shown) on single axis of PMF.

Manuscript received January 16, 1995; revised March 19, 1995. This work was sponsored by the Office of Naval Research Fiber Optics Technology Area Program.

The authors are with the Naval Research Laboratory, Optical Techniques Branch, Code 5670, Washington, DC 20375 USA.

IEEE Log Number 9413772.

For feed-through arrangements, a polarization-insensitive modulator loop configuration has been demonstrated for liquid crystals [15] and a Faraday rotator and mirror combination has been demonstrated with semiconductor optical amplifiers [16] but, in both cases, both axes of polarization are utilized. The polarization sensitivity of many modulators effectively polarize the input signal or effect each SOP differently and so cannot be used in these configurations. We note, however, that the OCLM design leads naturally to an alternate single polarization loop (SPL) configuration [12] [Fig. 1(b)], which has previously been used for elimination of polarization dependence of semiconductor optical amplifiers [17], [18]. With oppositely oriented 45° FR's located at ports 2 and 3, this SPL arrangement utilizes only a single axis of the PMF loop and delivers a constant (i.e., input SOP independent) optical output at port 4 for a return (or output) on a separate SMF. The feed-through configuration is important for long distance interrogation of remotely located sensors since no remoting length restriction is needed and signal degradation by copropagation with Rayleigh backscatter is avoided.

III. Jones Matrix Analysis

In the Jones matrix analysis of the OCLM, we consider an input optical electric field $\mathbf{E}_{\text{in}}$ with an arbitrary SOP

$$\mathbf{E}_{\text{in}} = \begin{bmatrix} E_x \\ E_y e^{i\varphi} \end{bmatrix}. \tag{1}$$

The transfer functions P_{ji} for the PBS from port i to port j is represented by

$$\begin{aligned} \mathbf{P}_{12} = \mathbf{P}_{21} = \mathbf{P}_{34} = \mathbf{P}_{43} &= \begin{bmatrix} 0 & 0 \\ 0 & 1 \end{bmatrix} \\ \mathbf{P}_{13} = \mathbf{P}_{31} = \mathbf{P}_{24} = \mathbf{P}_{42} &= \begin{bmatrix} 1 & 0 \\ 0 & 0 \end{bmatrix}. \end{aligned} \tag{2}$$

For the case of the SPL we must convert to the principle axes of PMF oriented at 45° relative to the input coordinate system, the conversion matrices at port 2 and 3, P2 and P3, respectively, are

$$\mathbf{P2}_{\substack{\text{out} \\ \text{in}}} = \mathbf{P3}_{\substack{\text{out} \\ \text{in}}} = \frac{1}{\sqrt{2}} \begin{bmatrix} 1 & \pm 1 \\ \mp 1 & 1 \end{bmatrix} \tag{3}$$

where "out" and "in" are relative to the PBS. With this particular choice of coordinate transformations and placement of FR's, we find that

$$\mathbf{P2}_{\text{out}}\mathbf{FR}_{+}(45°)\mathbf{P}_{21} = \begin{bmatrix} 0 & 0 \\ 0 & 1 \end{bmatrix}$$

and

$$\mathbf{P3}_{\text{out}}\mathbf{FR}_{-}(45°)\mathbf{P}_{31} = \begin{bmatrix} 0 & 0 \\ -1 & 0 \end{bmatrix} \tag{4}$$

which implies that only the y axes of the PMF loop is utilized. The FR matrix is

$$\mathbf{FR}_{\pm}(\theta) = \begin{bmatrix} \cos\theta & \mp\sin\theta \\ \pm\sin\theta & \cos\theta \end{bmatrix}. \tag{5}$$

where the direction of the FR magnetic field vector H is in the same (+) or opposite (−) direction to the light. The operations of the OCLM and SPL are then given by

$$\begin{aligned} \mathbf{F}(\text{OCLM}) &= \mathbf{P}_{12}\mathbf{FR}_{+}(90°)\mathbf{P}_{31} + \mathbf{P}_{13}\mathbf{FR}_{-}(90°)\mathbf{P}_{21} \\ &= \begin{bmatrix} 0 & 1 \\ 1 & 0 \end{bmatrix} \end{aligned} \tag{6a}$$

and

$$\begin{aligned} \mathbf{F}(\text{SPL}) &= \mathbf{P}_{42}\mathbf{FR}_{-}(45°)\mathbf{P2}_{\text{out}}\mathbf{P3}_{\text{in}}\mathbf{FR}_{+}(45°)\mathbf{P}_{31} \\ &\quad + \mathbf{P}_{43}\mathbf{FR}_{+}(45°)\mathbf{P3}_{\text{in}}\mathbf{P2}_{\text{out}}\mathbf{FR}_{-}(45°)\mathbf{P}_{21} \\ &= \begin{bmatrix} 1 & 0 \\ 0 & 1 \end{bmatrix}. \end{aligned} \tag{6b}$$

Now, for the beam returning from the OCLM, we adopt the convention [19] that a wave always propagates in the $+z$ direction. This is accomplished by a transformation from the incident coordinate system to the reflected system such the $x \rightarrow -x$ and $z \rightarrow -z$. The transformation is represented by the operator

$$\mathbf{R}\left\{ \begin{matrix} \overleftarrow{} \\ \overrightarrow{\begin{bmatrix} a \\ b \end{bmatrix}} \end{matrix} \right\} = \begin{matrix} \overrightarrow{} \\ \overleftarrow{\begin{bmatrix} -a^* \\ b^* \end{bmatrix}} \end{matrix} \tag{7}$$

where the arrow indicates the propagation direction. In our system

$$\vec{\mathbf{E}}_{\text{out}} = \mathbf{F}(\text{OCLM})\vec{\mathbf{E}}_{\text{in}} = \begin{bmatrix} \vec{E_y e^{i\phi}} \\ E_x \end{bmatrix} = \begin{bmatrix} -\overleftarrow{E_y e^{i\phi}} \\ E_x \end{bmatrix}. \tag{8}$$

Finally

$$\vec{E}^{*}_{\text{in}} \bullet \overleftarrow{E}_{\text{out}} = \begin{bmatrix} \vec{E_x} \\ E_y e^{i\phi} \end{bmatrix} \bullet \begin{bmatrix} \overleftarrow{-E_y e^{-i\phi}} \\ E_x \end{bmatrix} = 0 \tag{9}$$

demonstrates the orthoconjugate property of the OCLM return beam.

Note that for the SPL the input light can be completely depolarized without effecting modulator performance. Also, an alternate feedback design might be considered without orthoconjugate return where the loop 90° Faraday rotator can be replaced by a fiber twist. This case has the advantages of 1) lower system complexity (cost) since the PBS1 can be replaced with a polarization insensitive coupler, 2) very long fiber lengths can be used since birefringence fluctuations (and fiber reciprocity) are no longer of concern, and 3)

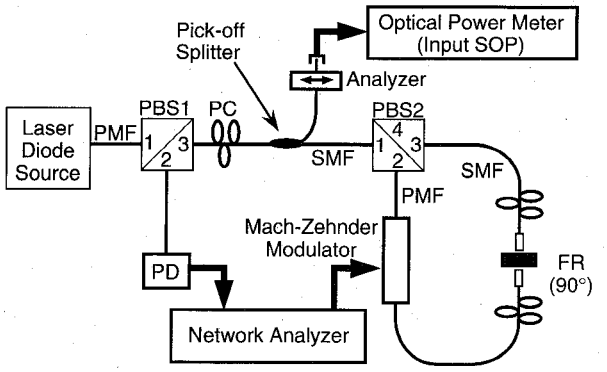

Fig. 2. Experimental arrangement of modulator in orthoconjugate configuration. PC: fiber loop polarization controller.

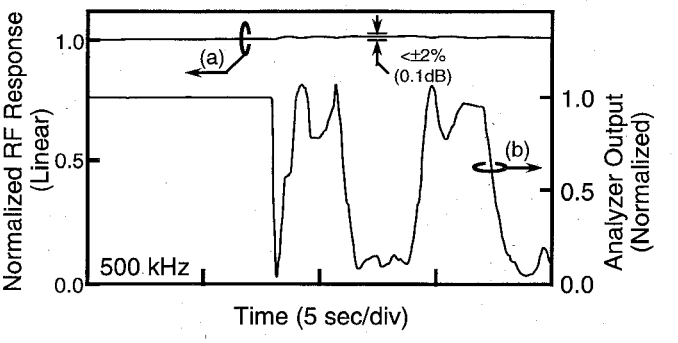

Fig. 3. Experimental verification. The upper trace (a) demonstrates the stability of RF modulation (500 kHz) while the input SOP is varied. The lower trace (b) is the SOP variation in the SMF input, where one corresponds to a linear SOP and zero corresponds to the orthogonal SOP and values between zero and one are arbitrary elliptical SOP's.

depolarized light still does not effect the modulator performance. However, this arrangement requires 6 dB more optical power for the same electrical system sensitivity since the coupler replacement introduces 3 dB optical loss in each direction.

IV. Modulator in the Loop

In an initial experimental implementation of this technique (Fig. 2), the polarization-sensitive modulator was a 1.3-μm Y-fed balanced bridge intensity modulator [20]. In this case, the modulator passes only the polarization that is modulated so that, assuming a y-axis orientation, the corresponding Jones matrices can be shown to be those of (6) modified by a scalar modulation factor—both the OCLM and the SPL remain independent of input SOP.

In place of a fiber-pigtailed Faraday rotator, a bulk Faraday rotator was accessed via a pair of gradient-index lenses pigtailed to SMF leads and spliced to the PMF output lead from port 3 of PBS2. This arrangement allowed for convenient access (removal) of the FR and fine adjustment in the loop lengths (below). However, to preserve the birefringence axes alignment of the loop PMF, the SMF leads were wrapped on fiber-loop polarization controllers [21]. Before inserting the FR, the birefringence axes were aligned by adjusting the polarization controllers to yield maximum photodetector (PD) response. The OCLM input SOP in the SMF was varied manually with another polarization controller and monitored by a pick-off splitter which diverted a small fraction of the light between PBS1 and PBS2 to a polarization analyzer and power meter. In Fig. 3 the upper trace (a) shows the demodulated RF power from the PD and the lower trace (b) is the input SOP variation in SMF. The maximum and minimum values in trace (b) correspond to linear SOP's parallel and perpendicular to the analyzer and the intermediate values represent arbitrary SOP's. The variation in RF power was found to be less than ± 0.1 dB.

This first modulator exhibited a 3-dB bandwidth of 870 MHz, so the frequency response of the configuration was measured. When the input SOP is set for only clockwise (CW) traversal of the OCLM loop, good frequency response is obtained out to 2 GHz. However, when both CW and CCW

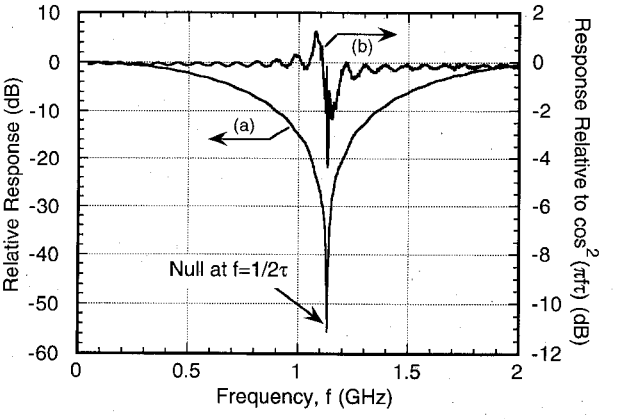

Fig. 4. Link frequency response. Trace (a) shows the response plotted for an input SOP that yields equal amounts of CW and CCW light as measured relative to only CW light in the loop. Trace (b) shows trace (a) response relative to $\cos^2(\pi f \tau)$ with τ set to 442 ps.

light are present in the OCLM loop, a large null is observed (Fig. 4). The null in response observed at 1.13 GHz is due to the modulator not being located half-way around the OCLM loop. That is, the modulated signals recombine at PBS2 with a relative time delay based on where the modulator is located in the loop. The relative frequency response of the system is given by

$$P_{\text{output}} \propto \{\sin(\omega t) + \sin[\omega(t+\tau)]\}^2 \propto \cos^2\left(\frac{\omega\tau}{2}\right) = \cos^2(\pi f \tau) \tag{10}$$

where τ is the time delay from the loop midpoint to the modulator midpoint. The null at 1.13 GHz corresponds to a time delay of 442 ps or 8.85 cm of optical fiber. After removal of the excess fiber on one leg of the loop and fine tuning (<1 cm) with stages that translate the gradient index lenses, the sharp null in the frequency response was completely removed (Fig. 5). What remained were any traveling-wave effects and any asymmetry in the modulator. It is noted that, as with other link throughput data presented in this paper, the link loss was measured to be commensurate with the modulator $V\pi$ and the received PD current.

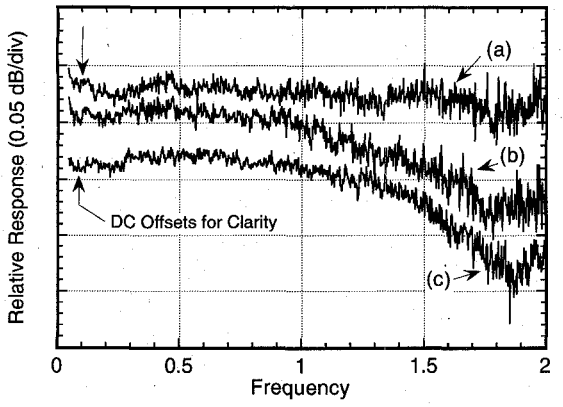

Fig. 5. Response versus frequency relative to copropagating RF and optical signals; trace (a) RF and optical copropagating (serves as a measure of system repeatability), (b) both co- and counterpropagating signals (single SOP setting), and (c) the case when the input SOP is adjusted so that the RF and optical waves are counterpropagating.

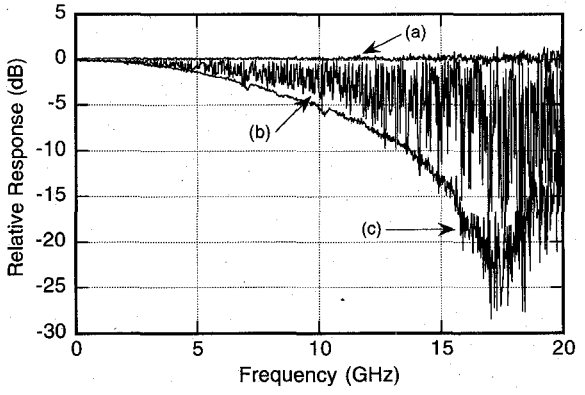

Fig. 6. Response versus frequency relative to copropagating RF and optical signals; trace (a) RF and optical copropagating (serves as a measure of system repeatability), (b) both co- and counterpropagating signals (input SOP varied using PC), and (c) the case when the input SOP is adjusted so that the RF and optical waves are counterpropagating (large dip is due to traveling-wave effects).

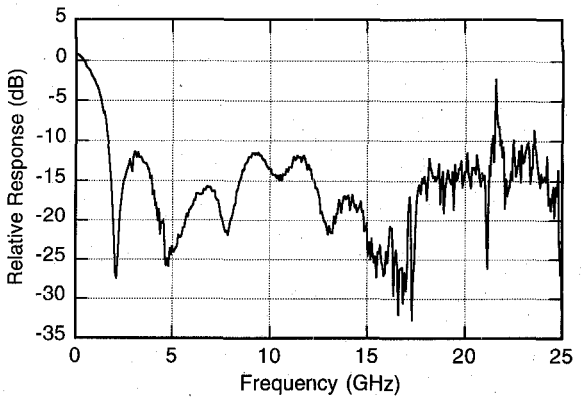

Fig. 7. Response of 40-GHz $LiNbO_3$ modulator for counterpropagating RF and optical signals (relative to copropagating). Response spike at ~21.5 GHz is due to PD resonance.

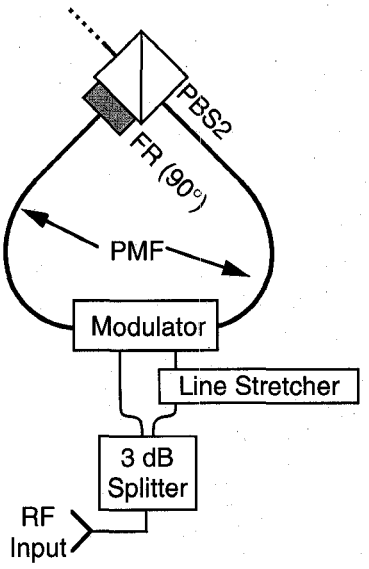

Fig. 8. Modulator feed arrangement for ultrawideband operation; the modulator is located at the midpoint of the OCLM and a line stretcher is used for microwave path matching.

V. Single-Drive Microwave Modulator

With the 90° FR attached directly to one of the loop ports [Fig. 1(a)], the CW and CCW circulating components of light in the OCLM travel on the same birefringence axis of the PMF. Therefore, any bidirectional modulator can be inserted in the OCLM and its operation will be independent of the input SOP. So in an effort to expand the bandwidth of this technique, a traveling-wave $LiNbO_3$ Mach-Zehnder modulator with operation to 18 GHz was substituted for the first modulator. However, traveling-wave devices require copropagation of the RF and optical waves as demonstrated by the measured results shown in Fig. 6. The top curve of Fig. 6 is taken relative to a previous curve for copropagating RF and optical waves and serves as a measure of system repeatability. The bottom curve is measured for the case when the input SOP is adjusted so that the RF and optical waves are counterpropagating in the OCLM loop. Input SOP variations yield widely varying response between the two curves. It is well known that traveling-wave microwave modulators exhibit directional dependence above some characteristic frequency, f_c, due to traveling wave effects [22]. The characteristic frequency and the null frequency (here observed at 17.3 GHz) yields information about the velocity mismatch between the RF and optical waves.

VI. Dual-Drive Microwave Modulator

The directional (input SOP) dependence can be removed, however, if a symmetric device is synchronously RF driven in both directions. The device used above is internally terminated and so can only be driven in one direction. Hence, another device was used to test this new dual-drive concept: an in-house traveling-wave $LiNbO_3$ Mach-Zehnder modulator having operation to 40 GHz [23]. As expected, the 40-GHz device exhibits inefficient modulation beyond 1 GHz when the RF and optical waves are counterpropagating (Fig. 7).

As described above, for ultrawideband operation the modulator is located at the appropriate midpoint of the OCLM and a line stretcher is used for corresponding microwave path matching (Fig. 8). At all microwave frequencies the light

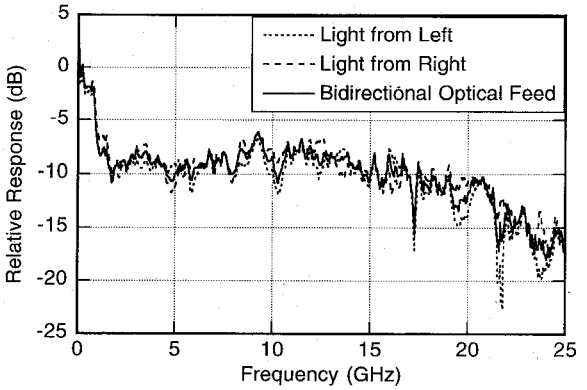

Fig. 9. Relative response versus frequency for (· · · · · ·) light from left input of modulator, (- - -) light from right input, and (—) typical bidirectional optical feed.

in either loop direction will interact with the corresponding copropagating microwaves. At frequencies less than f_c the light will interact with both the co- and counterpropagating microwaves. The response of the modulator will then be doubled at low frequencies but, when included in the OCLM, complete polarization independence is obtained.

This dual-fed ultrawideband technique was characterized for polarization sensitivity. For the $LiNbO_3$ device of Fig. 7, the polarization dependence (loop direction dependence) is substantially reduced (Fig. 9) out to 25 GHz. The response with bidirectional optical feed was found to always lie between the responses for optical feeds solely from the left or right inputs to the modulator. Compared to Fig. 5, the residual polarization dependence increases to as much as $\sim\pm 2$ dB for some frequencies. Upon close examination of corresponding time-domain data, these resonances are suspected to be due to both electrical reflections, associated with the modulator impedance mismatch (35 to 50 Ω), and due to optical reflections at the $LiNbO_3$-fiber interface. Additionally, the microwave power splitter was measured to have $\sim$0.5 dB splitting asymmetry across the 25 GHz band. Nevertheless, for select narrowbands the polarization dependence is almost completely removed ($<\pm 0.3$ dB) for both dual-fed modulators tested—indicating the potential of the technique.

VII. Summary

In summary, we have presented the orthoconjugating loop mirror and its implementation for removing polarization sensitivity in ultrawideband modulators. For low-frequency operation, the polarization sensitivity was easily reduced to ± 0.1 dB. For bulk modulators (not specifically designed for traveling wave operation), the polarization sensitivity was reduced to ± 0.15 dB out to 2 GHz. This technique effectively replaces polarization dependence with direction dependence and so has limited applicability to unidirectional traveling-wave devices. By utilizing bidirectional traveling-wave modulators, however, polarization sensitivity was reduced to $\pm$ 0.3 dB in narrowbands and $\sim\pm$ 2 dB from DC to 25 GHz. Improvements in polarization sensitivity are expected to accompany any improvement in modulator symmetry and reduction in optical and electrical reflections. The technique can be implemented in either a common input-output orthoconjugate configuration or a transmissive configuration. The loop mirror enables the system to passively operate independently of the evolution of the state of polarization over a singlemode fiber link between the source/detector and the sensing head. Thus, cost and complexity are reduced for new installations and existing installed singlemode fibers can be used for ultrawideband remote sensing.

Acknowledgment

The authors wish to thank I. N. Duling, III, A. D. Kersey, G. K. Gopalakrishnan for fruitful discussions and J. F. Weller for encouragement.

References

[1] D. W. Stowe *et al.*, "Polarization fading in fiber interferometric sensors," *J. Quantum Electron.*, vol. QE-18, pp. 1644–1651, 1982.
[2] K. H. Wanser and N. H. Safar, "Remote polarization control for fiber-optic interferometers," *Opt. Lett.*, vol. 12, pp. 217–219, 1987; and references therein.
[3] N. G. Walker and G. R. Walker, "Polarization control for coherent communications," *J. Lightwave Technol.*, vol. 8, pp. 438–458, 1990.
[4] A. D. Kersey, M. J. Marrone, and A. Dandridge, "Polarization diversity detection for fiber interferometers using active feedback control of output polarization-mode selection," *Opt. Lett.*, vol. 15, pp. 1315–1317, 1990.
[5] A. D. Kersey *et al.*, "Optimization and stabilization of visibility in interferometric fiber-optic sensors using input-polarization control," *J. Lightwave Technol.*, vol. 6, pp. 1599–1609, 1988.
[6] T. G. Hodgkinson *et al.*, "Polarization insensitive heterodyne detection using polarization scrambing," in *Dig. Conf. Opt. Fiber Commun.*, 1987 Tech. Dig. Series, Opt. Soc. Am., Wash., DC), 1987, Postdeadline paper 15.
[7] A. D. Kersey and A. Dandridge, "Monomode fiber polarization scrambler," *Electron. Lett.*, vol. 23, pp. 634–635, 1987.
[8] W. K. Burns and A. D. Kersey, "Fiber-optic gyroscopes with depolarized light," *J. Lightwave Technol.*, vol. 10, pp. 992–999, 1992.
[9] A. D. Kersey *et al.*, "Analysis of input-polarization-induced phase noise in interferomeric fiber-optic sensors and its reduction using polarization scrambling," *J. Lightwave Technol.*, vol. 8, pp. 838–845, 1990.
[10] W. K. Burns *et al.*, "Depolarized source for fiber-optic applications," *Optics Lett.*, vol. 16, pp. 381–383, 1991.
[11] M. M. Howerton and W. K. Burns, "Depolarized source for high power remote operation of an integrated optical modulator," *IEEE Photon. Technol. Lett.*, vol. 6, pp. 115–117, 1994.
[12] R. D. Esman *et al.*, "Technique to eliminate polarization sensitivity in fiber-optic transducers," in *Conf. Lasers and Electro-Optics*, 1993, vol. 11, OSA Tech. Dig. Series (Opt. Soc. Am., Wash., D.C.), pp. 2–3, 1993.
[13] M. Martinelli, "A universal compensator for polarization changes induced by birefringence on a retracing beam," *Opt. Commun.*, vol. 72, pp. 341–345, 1989.
[14] C. Edge and W. J. Stewart, "Measurement of nonreciprocity in single-mode optical fibers," in *Tech. Dig. IEEE Colloq. Opt. Fiber Meas.*, no. 1987/55, pp. 12/1–4, 1987.
[15] G.-K. Chang *et al.*, "Polarization-independent lightwave switch/pmodulator at 820 nm and 1300 nm for fiber-optic systems," *Electron. Lett.*, vol. 25, pp. 119–120, 1989.
[16] N. A. Olsson, "Polarization-independent configuration optical amplifier," *Electron. Lett.*, vol. 24, pp. 1075–1076, 1988.
[17] M. Sumida, "Polarization insensitive configuration of semiconductor laser amplifier," *Electron. Lett.*, vol. 26, pp. 1913–1914, 1990.
[18] L. F. Tiemeijer, "A single-pass single-amplifier polarization-insensitive semiconductor laser amplifier configuration," *J. of Quantum Electron.*, vol. 30, pp. 37–42, 1994.
[19] A. Yariv, "Operator Algebra for propagation problems involving phase conjugation and nonreciprocal elements," *Appl. Optics*, vol. 26, pp. 4538–4540, 1987.
[20] United Technologies Photonics Model FYBBM, APE Y-Fed Balanced Bridge Modulator, Bloomfield, CT 06002.
[21] H. C. Levevre, "Single-mode-fiber fractional-wave devices and polarization controller," *Electron. Lett.*, vol. 16, pp. 778–780, 1980.

[22] R. G. Walker, "High-speed II–V semiconductor intensity modulators," *J. Quantum Electron.*, vol. 27, pp. 654–667, 1991.
[23] G. K. Gopalakrishnan *et al.*, "Electrical loss mechanisms in travelling wave $LiNbO_3$ optical modulators," *Electron. Lett.*, vol. 28, pp. 207–209, 1992.

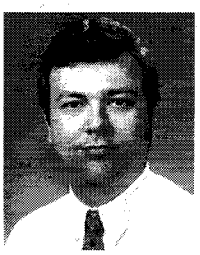

R. D. Esman (S'82–M'85) received the B.A. degree, *magna cum laude*, in physics and mathematics from Kalamazoo College, Kalamazoo, MI, in 1981. In 1980, he interned at Oak Ridge National Laboratory, Oak Ridge, TN, where his research included characterization and passivation of polycrystalline Si solar cells. He received the M.S. and D. Sc. degrees in electrical engineering from Washington University, St. Louis, MO, in 1983 AND 1986, respectively. His doctoral thesis research was in the areas of fabrication, large-signal analysis, and characterization of high-speed electroabsorption avalanche photodetectors.

He joined Naval Research Laboratory, Washington, D.C, in 1986, where he began work in the fields of high-speed optoelectronics, optical-microwave interactions, semiconductor laser noise and spectral characteristics, and fiber-optics. He was with NIST, Boulder, CO, from 1990–1991, where he studied high-speed coherent optical transmission and measurement techniques at NTT Transmission Systems Laboratory, Yokosuka, Japan. He is presently Head of the Fiber-Optic Microwave Signal Processing Section at NRL, which is involved in RF array beamforming, remote sensing, photodetector nonlinearities, and picosecond optical probing.

Dr. Esman is a member of Sigma Xi and the Optical Society of America.

M. J. Marrone received the B.S. degree from the University of Notre Dame, Notre Dame, IN, the M.S. degree from the University of Pittsburgh, Pittsburgh, PA, and the Ph.D. degree from the Catholic University of America, Washington, D.C., all in physics.

He joined the Naval Research Laboratory , Washington, D.C., in 1961. His research interests have included self-trapped exciton luminescence in alkali halides and EPR in the excited state of the self-trapped exciton, picosecond phenomena in gas phase photolysis, and radiation-induced luminescence effects i optical fibers. His recent work concerns the polarization properties of single-mode fibers and the effects of polarization in fiber-optic sensors.

Dr. Marrone is a member of Sigma Xi and the Optical Society of America.